

Investigation of flow and heat transfer at the surface of a single circular cooling fin

S Z Sapozhnikov, V Y Mityakov, A V Mityakov*, A A Gusakov, M A Grekov, V V Seroshtanov

Peter the Great Saint-Petersburg Polytechnic University,
Polytekhnikeskaya Str., 29, St. Petersburg, Russian Federation

*Corresponding author E-mail: mitiakov@spbstu.ru

Abstract

All heat transfer processes are connected with flow structure. It is important to know both heat transfer and flow characteristics. For the first time it is proposed to connect Particle Image Velocimetry (PIV) method with gradient heat flux measurement and thermal imaging for complex study of hydrodynamics and heat transfer at the surface of a single circular cooling fin. The hollow fin is heated with saturated water steam; meanwhile its isothermal external surface simulates the ideal fin. Flow and heat transfer at the surface of the solid fin of the same size and shape, and made of titanium alloy is investigated in the same regimes. Gradient Heat Flux Sensors (GHFS) were installed at different places of the fin surface. Velocity field near the fin, temperature field at the surface of the fin and heat flux were obtained. Comprehensive method including heat flux measurement, PIV and thermal imaging allows to study the flow and heat transfer at the surface of the fin in real time regime. The possibility of complex study of flow and heat transfer for non-isothermal fins is shown.

Keywords: PIV; heat exchange; heat flux measurements; circular fin.

1. Introduction

A number of recuperative heat exchanger designs use finned cylinder tubes to increase the heat transfer surface. However, despite wide prevalence of finned heat exchangers, there is no universal method for calculation. This fact is due to the uneven distribution of the heat transfer coefficient at the surface of the fin [1-4]. It is also difficult to ensure the exact angle between the velocity vector and the tube axis [5]. Since heat transfer and hydrodynamics are closely interrelated, it is important to study them simultaneously. All of the above served as a basis for this present research.

Until recently, heat transfer and flow usually have been studied in separate experiments. Techniques and equipment for experimental research of fluid mechanics are diverse and approved. However, the investigations of heat transfer at different surfaces are troubled by the unavailability of heat flux sensors with required response time. Due to this situation, the temperature is often measured and the heat transfer coefficients are calculated from similarity equations. For a more accurate comparison of flow and heat transfer, a combination approach that includes simultaneous measurement of heat transfer parameters (heat flux per unit area and heat transfer coefficient) using unique gradient heat flux sensors (GHFS), velocity fields using PIV method and temperature fields visualized by thermal imaging is proposed.

2. Investigation method

Since the method used includes several complex technologies, it is necessary to explain the specifics of each of them separately.

2.1 Heat flux measurement

Heat flux per unit area is measured by a unique GHFSs with response time of $10^{-8} \dots 10^{-9}$ s. GHFSs have been developed, created and integrated into the laboratory and industrial experiment at the "Thermophysics of Power Units" department of Peter the Great St. Petersburg Polytechnic University, Russia since 1996. Such small response time of the GHFS practically makes them the non-inertia instrument for study most heat transfer types [7-9]. Figure 1 shows the scheme (a) and the general view (b) of the battery GHFS based on bismuth single crystals, which are used in experiments of this study. The choice of GHFS type is due to the low surface temperatures and small temperature drop. Figure 1(c) shows three GHFSs mounted at the circular fin.

The action of GHFS is based on Seebeck's transverse effect: when a heat flux passes through a plate with anisotropy of thermophysical and thermoelectric properties, the thermopower arises proportional to heat flux value. Five sensors are used in the experiments; the dimensions of three GHFSs in plan are of 2×2 mm, the fourth sensor is of 4×7 mm and the fifth one is of 5×5 mm. Sensors are 0.2 mm thick with volt-watt sensitivity of about 10 mV/W. The GHFSs are mounted with a special compound with high thermal conductivity. Wires soldered to the GHFSs are led along the fin and the cylinder, and at some points are attached to the cylinder with the help of glue. In addition, in the selected range of regimes, the velocity did not exceed 15 m/s.

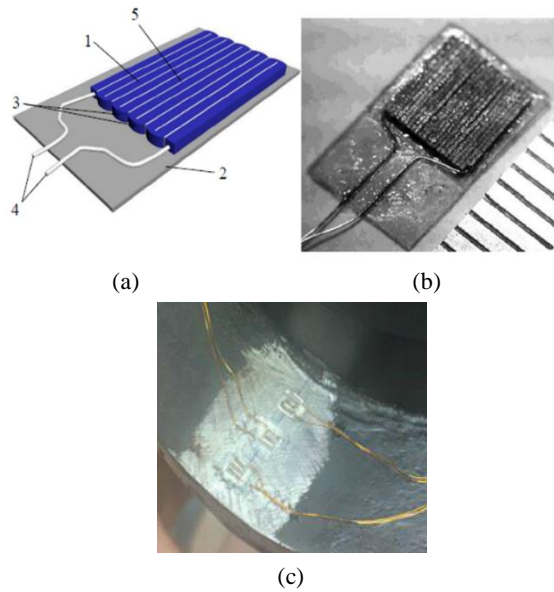


Fig. 1: Scheme (a), general view (b) of the GHFS and GHFSs mounted at the fin (c). Figures denote: 1 – anisotropic bismuth strips; 2 – silica substrate; 3 – pure bismuth junctions; 4 – current outputs; 5 – lavsan spacers

2.2 PIV method

PIV technology makes it possible to visualize the flow near the surface of the fin by non-invasive method, which allows to record instantaneous velocity fields in plane of the laser sheet. Principle of any PIV system operation is that the tracers are fed into the airflow: fine particles (with a diameter of $2 \dots 3 \mu\text{m}$), which are illuminated by a laser beam reshaped by a lens system into the laser sheet. In this case, the supply of tracers is provided by a fog machine. A digital camera at moments of flashes fixes the image of tracers. POLIS system [10] renders possible to adjust the supply of tracers and the frequency of photographs under the flow regime. All photos are processed in the ActualFlow program, which gives the velocity field for each time step. Correlation methods of image processing to obtain particle shifts are used.

2.3 IR imaging

To measure temperature of the fin, a thermographic camera FLIR P640 is used. Its software allows it to produce powerful temperature analysis and automatic reporting. In addition, the camera has several aiming points, which enables the measurement of temperature at the places where GHFSs are installed.

3. Experimental model

The first model of finned cylinder of 66 mm in diameter and of 600 mm in length is made from a steel sheet of 0.1 mm thick. Two circular fins with external diameter of $D = 146 \text{ mm}$ are mounted at the cylinder. The first fin is hollow and it simulates “ideal” (isothermal) fin while the second is made of titanium alloy with thermal conductivity of about $k = 9 \text{ W/(m}\times\text{K)}$. On the other hand, the second model of the finned cylinder is made in similar fashion but the outer diameter of the fins is 186 mm. The GHFSs are mounted at the fins surface (Figure 2). Both models are heated with saturated water steam under the atmospheric pressure; therefore cylinder temperature is close to 100°C . The cylinder is turned around its axis, which allows the sensor movement in the circumferential direction. For the “ideal” fin surface temperature $T_w = \text{const}$ for all $0 \leq \varphi \leq 180$ (Figure 2(a)), and for the fin made from titanium alloy, T_w depends on the fin height and the angular coordinate: $T_w = (b, \varphi)$ (b — present-position data, mm; $0 \leq b \leq B$).

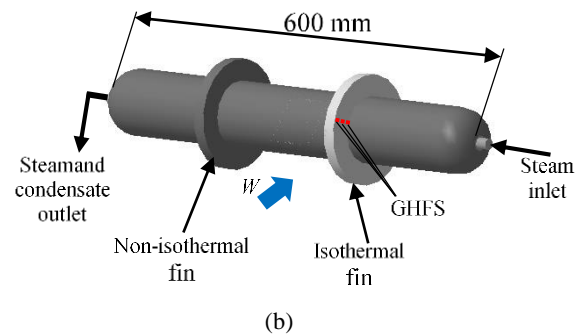
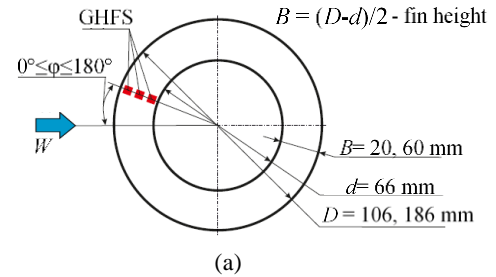


Fig. 2: Scheme (a) and general view (b) of the finned cylinder model.

The experiments are carried out in the subsonic wind tunnel of the “Thermophysics of Power Units” department of Peter the Great Saint-Petersburg Polytechnic University (Figure 3).

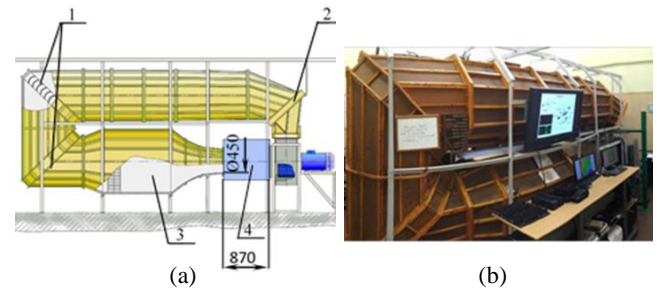


Fig. 3: Scheme (a) and photo (b) of the wind tunnel: 1 - turning vanes, 2 - heat exchanger, 3 - settling chamber with honeycomb, 4 - Eiffel chamber.

This wind tunnel has the following three features:

- The use of semiconductor-controlled rectifier (SCR's control) drive and reverser of the fan allows experiments to be produced at flow speed not exceeding of $0.1 \dots 0.2 \text{ m/s}$.
- The heat exchanger (cooler) that is connected to a cold water supply system ensures a long operation of the tunnel in air, which practically does not change its temperature (the spread of the values is $\pm 0.1 \text{ }^\circ\text{C}$).
- Eiffel camera allows the use of PIV system without appreciable dispersion of tracers.

4. Results

Research is carried out for Reynolds number $\text{Re} = \frac{Wd}{\nu}$, where W

– average flow velocity, m/s; d – diameter of cylinder, m; ν – kinematic viscosity of air, m^2/s . On Figure 4 dependence of average (over the fin's length) heat transfer coefficient on Reynolds number for isothermal (a, c) and non-isothermal (b, d) fins of different heights is shown. It can be seen that coefficient of heat transfer decreases in interval of $\varphi = 120 \dots 180^\circ$. This can be explained by the fact that the nature of flow is such that a vortex is formed behind the midsection of the cylinder and there is a stagnant zone near the cylinder.

Local heat transfer coefficient is defined as:

$$h_{\phi} = \frac{q_{\phi}}{T_f - T_w}, \text{ (W/ (m}^2 \times \text{K))}$$

(q_{ϕ} – local heat flux, W/m²; T_f – flow temperature, K; T_w – surface temperature, K)

Flow temperature is measured by multifunction instrument “testo-435-4” and fin surface temperature sensed by IR imaging.

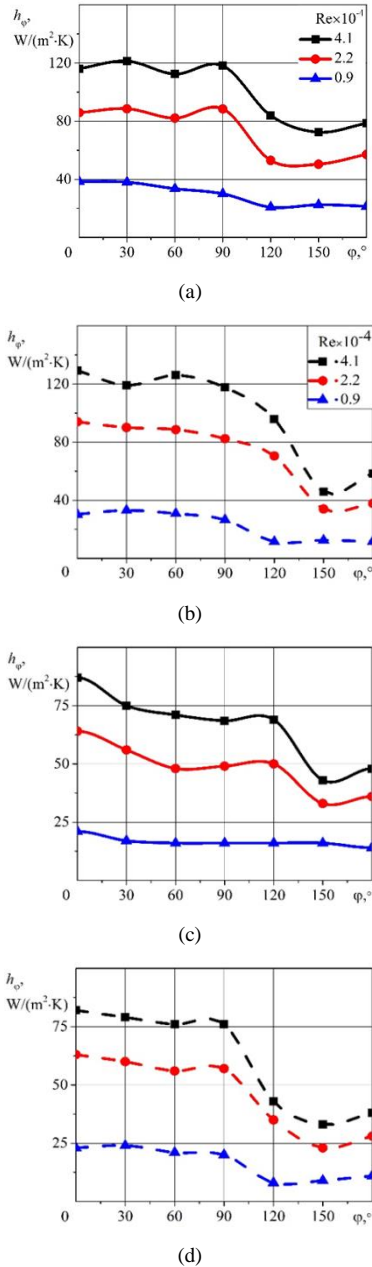


Fig. 4: Dependence of average heat transfer coefficient on the angle of rotation ϕ : (a) and (b) – for $B = 20$ mm, (c) and (d) – for $B = 60$ mm.

Local heat flux is measured by GHFS and equals to:

$$q_{\phi} = \frac{E}{S_0 \cdot F}, \text{ (W/ m}^2\text{)}$$

(E – thermopower, mV; S_0 – volt-watt sensitivity, mV/W; F – GHFS area, m²)

The Signal E is measured with a digital voltmeter. The sensitivity is known according to a predetermined calibration with measurement uncertainty of calibration of 1.3 %. Figure 5 illustrates the velocity fields near the fins of different heights. The figure shows

that stream pattern around the fin of 20 mm high is different from the flow near the fin of 60 mm high.

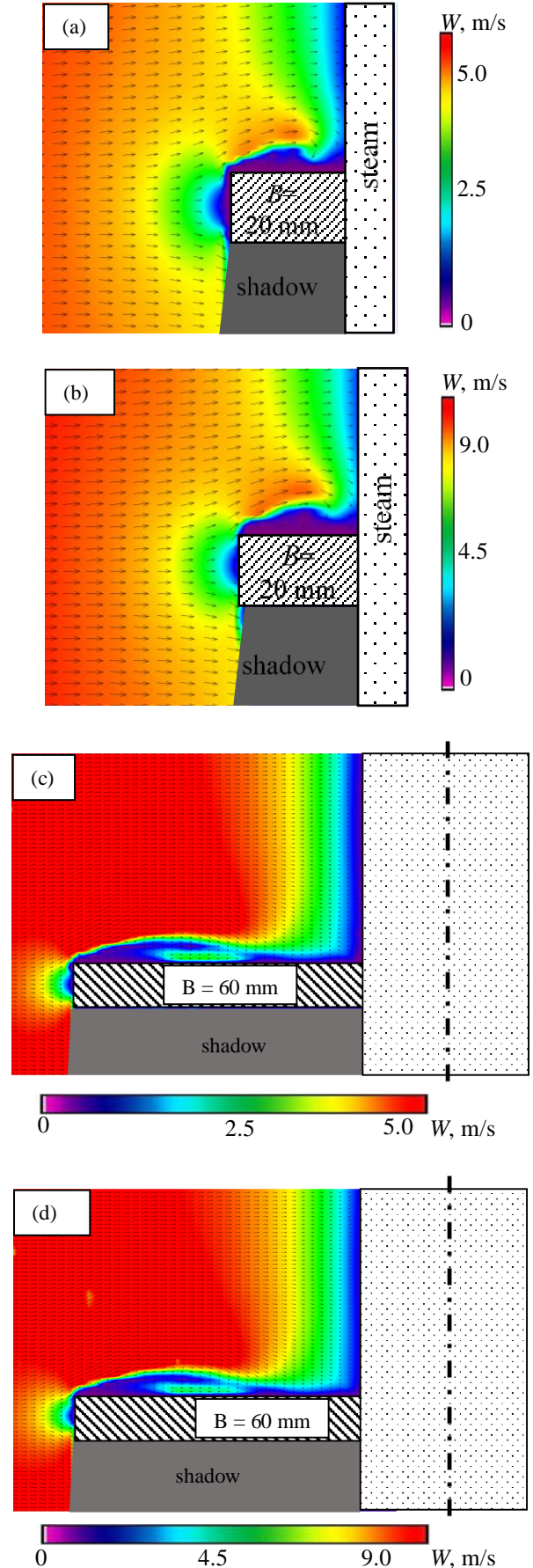


Fig. 5: Velocity fields near the fin: a,b - for $Re = 2.2 \times 10^4$; c,d - for $Re = 4.1 \times 10^4$

Vectors show the flow direction in plane of light sheet, and color show the speed value. The PIV-experiments for 60-mm-high fin show the presence of a vortex formed by flow separation. This vortex is absent at the “small” fin. Additionally, the influence of yaw angle is detected on flow and heat transfer. Thus, in Figure 6, the time-average velocity fields near the fins, flowing at yaw angle $\beta = 5 \dots 15^\circ$ are presented.

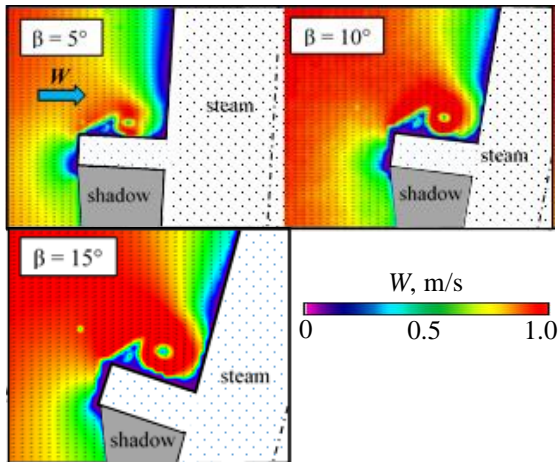


Fig. 6: Velocity fields near the fin: a,b - for $Re = 2.2 \times 10^4$; c,d - for $Re = 4.1 \times 10^4$

With a non-cross flow around a “small” edge, a vortex is formed. This vortex increases with increasing yaw angle. Furthermore, the proposed method allows to obtain three-component fields of heat transfer coefficient. For example, Figure 8 shows three-component distribution of heat transfer coefficients for non-cross flow. Since the flow is not symmetrical, the figure shows the distributions of these coefficients at the over-type (I) and under-type (II) surfaces of the fin. To verify the obtained data, the heat flux at various points is measured 2 to 3 times. This work repeats the studies in [11,12] based on the methods, however the use of thermal imager makes it possible to solve a problem connected with the investigation of heat transfer at any non-isothermal surface.

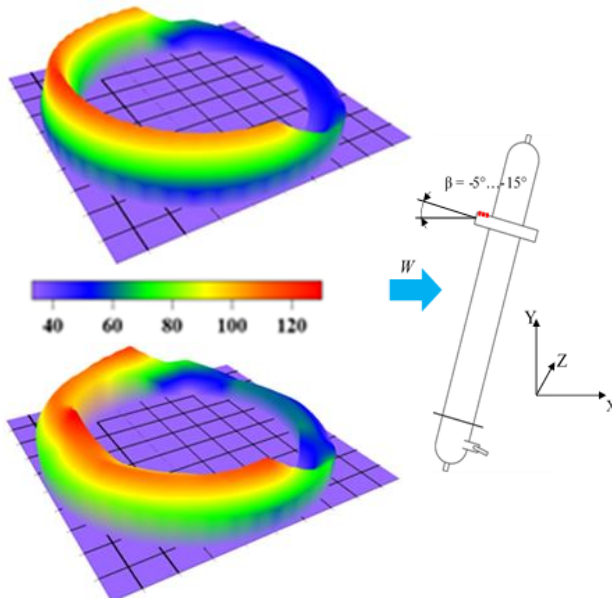


Fig. 7: Three-component distribution of heat transfer coefficients

5. Conclusion

The proposed technique, including superposition of gradient heat flux measurement, PIV diagnostics and thermal imaging, allows the study of flow and heat transfer at the surface of a single circular cooling fin. The presence of vortices over the fin is confirmed

and the influence of the height of the fin on flow structure is revealed. The influence of yaw angle on the flow and heat transfer is identified. Distribution of local heat transfer coefficient for “ideal” and real fins is different.

References

- [1] Webb RL & Kim N (2005), *Principles of Enhanced Heat Transfer*. Taylor & Francis Group.
- [2] Hamakawa H, Matsuoka H, Hosokai K, Nishida E & Kurihara E (2014), Characteristics of aerodynamics sound radiated from two finned cylinders. *ASME 2014 Pressure Vessels and Piping Conference*.
- [3] Sparrow EM, Gorman JM, Friend KS & Abraham JP (2013), Flow regime determination for finned heat exchanger surfaces with dimples/protrusions. *Numerical Heat Transfer, Part A: Applications*. 63(4), 245–256.
- [4] Bansal M (2014), *Experimental and numerical investigation of three equispaced cylinders in cross-flow*. University of Waterloo, Canada.
- [5] Sumner D (2013), Flow above the free end of a surface-mounted finite-height circular cylinder: A review, *Journal of Fluids and Structures* 43, 41–63.
- [6] Sparrow EM & Samie F (1986), Heat transfer from a yawed finned tube. *Journal of Heat Transfer* 10, 479–481.
- [7] Sapozhnikov SZ, Mityakov VY & Mityakov AV (2013), *Gradient heat flux measurement fundamentals*. St. Petersburg State Polytechnical University, Saint Petersburg (in Russian).
- [8] Korotkov A, Loboda V, Makarov S & Feldhoff A (2017), Modeling thermoelectric generators using the ANSYS software platform: methodology, practical applications, and prospects. *Russian Microelectronics*.
- [9] Korotkov A, Loboda V, Feldhoff A & Groeneveld D (2017), Simulation of thermoelectric generators and its results experimental verification. *IEEE, Signals, Circuits and Systems (ISSCS) International Symposium*.
- [10] Akhmetbekov YK, Bilsky AV, Markovich DM, Maslov AA, Polivanov PA, Tsyryul'nikov IS & Yaroslavl'tsev MI (2009), Application of "POLIS" PIV system for measurement of velocity fields in a supersonic flow of the wind tunnels. *Thermophysics and Aeromechanics* 16(3), 325-333.
- [11] Gusakov AA, Kosolapov AS, Markovich DM, Mityakov AV, Mityakov VY, Mozhayskiy SA & Nebuchinov AS & Sapozhnikov SZ (2014), Simultaneous PIV and gradient heat flux measurement of a circular cylinder in cross-flow. *Applied Mechanics and Materials* 629, 444-449.
- [12] Mityakov A, Mityakov V, Sapozhnikov S, Gusakov A, Bashkatov A, Seroshtanov V, Zainullina E & Babich A (2017), Hydrodynamics and heat transfer of yawed circular cylinder. *Int. J. Heat Mass Transf.* 115, 333-339.